

Acceleration-Retardation of Calcium Carbonate Scale Deposition under Static Electric Potential

Bisweswar Ghosh¹

Muhammad Ihtsham Hashmi²

Liyang Sun³

Petroleum Engineering Department.

The Petroleum Institute. Abu Dhabi. UAE.

Email; bghosh@pi.ac.ae

Abstract—Calcium carbonate scale nuclei are found to carry residual surface charges. Depending on the chemistry of the solution and physical condition they are exposed to, they display positive or negative surface potential as seen in ζ -potential measurement. It is expected that static electric potential may have impact on calcite nuclei and affect their deposition rate on the metal surface. This research investigated the possibilities of controlling calcium carbonate scale deposition during pipe flow by applying static electrical potential taking advantage of their surface charge. Detail laboratory experiments were performed both at static and at dynamic conditions under variable temperatures and potential differences. The deposition rate is indirectly measured through pressure rise across the loops. It is seen that the deposition rate is accelerated at the cathode and retarded at the anode loop. Retardation is more pronounced compared to acceleration and the impact of static potential is higher at higher temperature. With the help of ζ -potential and flow study data it is concluded that the deposition at cathode is due to the initial unstable vaterite (CaCO_3) structure with a net positive charge. It is also inferred that even though it cannot be prevented completely in the anode, the deposition of CaCO_3 scale can be delayed significantly by applying static DC potential and converting the metal flow line into an anode.

Keywords—*Electrostatic Scale remediation, Calcium Carbonate, Static potential. Scale inhibition*

I. INTRODUCTION

Calcite is the most common and stable polymorph of calcium carbonate (CaCO_3) and the major cause of scale deposition in most industries that deals with hard water. The other polymorphs of CaCO_3 are aragonite and vaterite, which are mostly seen as the intermediate product during the crystallization process to calcite. Calcite scale nucleation, growth and deposition is a complex process which depends not only on the water chemistry but also on the physics and mechanics of the system through which it flows. If not checked at the early stage the problem may rapidly exacerbate and the ever growing layers of rock-like

deposits eventually block the flow conduits, leading to system shut down.

Like all crystals, CaCO_3 crystals show defects in one of the following ways (Moulin and Roques, 2003); (i) Structural defects of the crystal lattice due to random substitutions of one of the lattice ions by a foreign ion or random omissions of native ions leaving an empty place in the crystal lattice. (ii) Exchange of ions between the crystal lattice ions and the ions in solution, even if the ions are not of comparable sizes. (iii) Reactions such as hydrolysis or protonation on the surface with constitutive ions. With these surface defects, a net residual surface force may result; The very small in absolute term, compared to the volume forces such as gravity, inertia etc.... it could be substantial when surface/volume ratio of the crystal is high as in the case of initial nucleation and growth stages and also under an electrical field.

Calcite crystal formation occurs from amorphous calcium carbonate, via the formation of individual vaterite which subsequently transforms themselves to calcite via a dissolution and re-precipitation mechanism, controlled by the surface area (Rodriguez-Blanco et al, 2011) system pH and presence of impurities (Rodriguez-Blanco et al, 2012). This is observed when the initial solution pH is basic and at neutral pH the transformation to calcite occurs through direct transformation of amorphous into calcite (Bots et al, 2012).

The unit cells of vaterite, calcite and aragonite crystalline structures are shown in Figure-1 (Blanco-Gutierrez et al. 2014). It can be seen that the average of Ca/CO_3 ratio per unit cell is largest in vaterite followed by aragonite and calcite. The charge density of calcium ions (ions per nm^2) in different crystalline planes of calcium carbonate polymorphs presented in Table-1 (Falini et al. 2000) support this observation.

Dynamic deposition of CaCO_3 crystals observed under AFM revealed that under normal condition the growth occurs in a layer-by-layer fashion by the forward motion of monomolecular steps of 0.3 ± 0.1 nm thickness which is attributed to the excess surface charge on the crystal nuclei noticed during zeta and surface potential measurements (Hillner et al, 1992). These surface electrical properties of CaCO_3 nuclei

are seen to be dependent on the pH and concentration of Ca^{2+} and CO_3^{2-} ions in solution in which they are subjected to precipitation. Zeta potential of CaCO_3 precipitated from a solution with excess Ca^{2+} is found to be positive and the opposite is measured when the solution has excess CO_3^{2-} . Zeta potential measured in equimolar solution seen to be slightly positive and after approximately 30 min changed to negative potential (Chibowski et al, 2003).

From the above discussion it is evident that whether due to the surface defect or due to the dissimilar surface charge distribution of different allotropes the surface electrical properties of the nascent suspended crystals may play a significant role during the nucleation, crystallisation and deposition process of calcite scaling.

The objective of this work is to take advantage of this excess surface charge of the nascent crystal units and study:

1. The acceleration/ retardation the calcite scale deposition rate under static electric field in static and flowing condition.
2. To find an explanation of the above through the Zeta potential measurements.
3. The possibility of applying electric field in arresting scale deposition in a flow conduit.

With the above objectives static jar tests were conducted as base experiments in order to understand the charge bearing properties of nascent CaCO_3 crystals under the influence of static DC potential, followed by a series of studies under dynamic conditions, under various voltage and temperature on a specially designed flow system. The underlying mechanisms are explained through the time dependent Zeta potential values.

II. MATERIALS AND METHODS

A. Characterization of ionic nature of calcium carbonate scale nuclei through jar test

These tests were designed in a fashion similar to half cells, however no current flow was allowed (Figure-2). Two graphite electrodes were placed in two separate 250 ml beaker and added 100 ml solution each of Na_2CO_3 and CaCl_2 (both at 2000 ppm concentration) and applied a DC potential difference of 5 volts across the electrodes. Similar experiments were repeated with increasing voltages i.e., 10, 15 & 20 volts. Reaction and crystal deposition was allowed for a long time till the deposition was visibly apparent.

B. Zeta Potential Measurements

Zeta PALS (Brookhaven Instruments) with phase analysis light scattering technique was used to measure the time dependent Zeta potential values of CaCO_3 crystals. The instrument uses He-Ne laser as a light source and it measures the electrophoretic mobility of charged colloidal suspensions. The cell was filled with 50:50 mixture of 1000 ppm solution of CaCl_2 and 1000 ppm solution of Na_2CO_3 , resulting in final

concentration of 500 ppm of Ca^{2+} and CO_3^{2-} each in the cell. Zeta potential was measured at frequent interval. Another set of experiments were conducted with increasing CaCl_2 to Na_2CO_3 ratio.

Electrophoretic method is used in which the suspended solid particles move with respect to the liquid by ensuring its electrophoretic transport in an electric field and measuring its limiting velocity.

C. Scale deposition under flowing condition

This set of experiments was conducted in a specially designed set up, description of which is given below (Figure-3). The setup was consisting of two high precision constant flow rate pumps (ISCO 100D), to inject two scale forming solutions.

Two stainless steel floating piston-cylinders, having capacity of 2000 ml each, connected to the pumps to inject CaCl_2 and Na_2CO_3 solutions separately, and comingled prior to the entry into two test coils after traveling through a larger diameter mixing tube. Arrangements were made to apply the DC potential across the test loops, using a DC power supply. Back pressure valves were introduced at both ends to equalize flow rate from the test loops.

Differential pressure transducers as depicted in the figure were installed across the inlet and outlet of each test loop, to measure real time pressure difference across the test loops. Higher temperature was maintained using electric heating jacket with thermostat regulators. Two identical stainless steel coiled tubes, each of 10 ft long and $\frac{1}{8}$ " in ID, were used as test loops connected to the solution cylinders and the back flow regulator at the other electrically isolated with plastic tubes. Test loop marked A was connected to the negative terminal of the power source (cathode) and the second test loop marked B was connected to the positive terminal of the power source (anode).

The flow experiments were performed both at room temperature and at elevated temperature of 90oC, under the influence of different static potentials applied across the test sections. 2000 ppm solution of CaCl_2 is placed in Cylinder-A and 2000 ppm solution of Na_2CO_3 in Cylinder-B, resulting in final concentration of 1000 ppm of Ca^{2+} and CO_3^{2-} in the mixed brine. The following flow studies are conducted:

D. Scale deposition studies at 25 oC (Set A)

Four runs were performed under this experiment; without application of static potential in test A1, and rest of experiments with 20V, 40V, and 60V in test A2, A3 and A4 respectively. Cylinder-A, filled with 2000 ppm solution of CaCl_2 and Cylinder-B, filled with 2000 ppm solution of Na_2CO_3 solution were injected simultaneously into the test section with the help of the pumps at a constant flow rate of 1ml/min.

1. Both the solutions entered to the test loops via a mixing port.

2. Differential pressure (DP) across the test loops began to rise after certain time due to scale deposition and narrowing of tube inner diameter. DPs were constantly monitored and recorded.
3. Flow was continued for 30 hours or rise of 500 psi DP whichever was earlier. Shaw tooth pattern DP was observed due to deposition and flushing of soft deposits.
4. No DC potential was applied for test A1, whereas static potentials of 20, 40 and 60 volts were applied across the test loops in the Test Run A2, A3 and A4, respectively.

E. Scale deposition studies at elevated temperature (Set B)

These experiments were performed at 90 oC. Rest of the procedure remained similar to the above and designated as B1 (without application of static potential) and with application of 20V, 40V, and 60V designated as B2, B3 and B4 respectively.

III. RESULTS

A. Static Scale Deposition

Condition of the graphite electrodes before and after CaCO_3 scale deposition is shown below in Figure-4 A & B respectively. Though deposition of scale on cathode is clearly visible on naked eyes, a confirmatory test was conducted with a drop of HCl on the electrodes. It is clearly evident from the amount of effervescence and the complete solubility of the deposited materials and lack of response of HCl on anode rod confirms that all the scale deposition occurred on the cathode only and the scales are CaCO_3 .

From this observation it is obvious that CaCO_3 scale nuclei are carrying a net positive charge on their surface and getting attracted towards the cathode.

B. ζ -Potential Studies

The results obtained from the ζ -Potential measurements are presented in Figure 5 & 6. ζ -Potential is the reflection of the surface charges which arises from the electric shear stress occurring between the fixed layer and the diffused layer, when solid particle is moved relative to the liquid. Figure-5 shows that the ζ -Potential of freshly precipitated CaCO_3 from a super-saturated mixture of Na_2CO_3 and CaCl_2 are close to zero at the instant of mixing of two solutions. Within few minutes it turned to positive, peaked at 5 minute and finally changed to a relatively large negative value. The results presented in this figure are the average of five experiments conducted at similar conditions. Thus there is little doubt that ζ -Potential of CaCO_3 is a time dependent phenomena. In the beginning of its formation, the crystal lattice does not carry any net residual charge, possibly due to unstructured agglomeration of unit crystal cells. The agglomerate then develop a crystal structure with a net positive charge which eventually changes to a net

negative charge possibly due to changes of its crystal morphology. This observation is similar to Hołysz et. al.(2002) who studied the effects of permanent magnetic fields on Zeta potential with equimolar concentration of Na_2CO_3 & CaCl_2 and in-situ precipitation of CaCO_3 as a function of time, under the exposure of magnetic fields. It was found that irrespective of exposure time, zeta potential under N-S magnetic field is always positive which is decayed down to a negative value once the magnetic exposure is removed.

In Figure 6 we present the change of ζ -Potential due to incremental presence of Ca^{2+} in the solution. The results are obtained within 2–2.5 min of mixing the solution and are average of 5 experiments at similar conditions. It is evident from this figure that increased presence of CO_3^{2-} reduced the ζ -Potential towards negative while it turned towards neutral potential with increased presence of Ca^{2+} in the solution. It is deduced from this observation that the so called PDIs (potential determining ions) in case of CaCO_3 in solution are Ca^{2+} and CO_3^{2-} , supporting the observation made by Pierrea et al (1990).

C. Dynamic Scale Deposition Studies

Results of the experimental Set-A (at 25 oC) and Set-B (at 90 oC) are given (in the form of time versus rise of differential pressure across the cathode and anode flow loops) in Figure-7 through 14. The data on the onset of scale deposition on cathode and anode loops at different temperature and potential differences are given in Table-2.

As the data table and Figure-7 show, at 25 oC when no DC potential is applied (blank test), the onset of scale deposition is about 450-460 minutes. Scale deposition started on both the loops at about the same time, as per expectation. Near complete blockage happened near 900 minutes. Several Shaw tooth are observed during this rise of pressure, possibly due to erosion of loosely bound deposited scale materials. Since we are interested on the onset of scaling, henceforth we would not consider tube blocking time or pressure. The ΔP pattern in the subsequent experiments conducted at low temperature under potential difference (PD) of 20, 40 & 60 volts are presented in Figure 8, 9 & 10. The test run with a static potential of 20 volts applied across the anode and cathode loops show significant difference in deposition kinetics. Scale deposition is delayed in anode loop to 640 min, which is 42% more delayed compared to that of the blank test whereas, it is accelerated in the of cathode loop by 29% (onset at 320 min).

In tests A3 at static potential of 40 volts, the deposition kinetics in the cathode loop is further accelerated (33 % faster than blank run) however the anode loop it shows less effectiveness in delaying the onset, compared to the 20 volts PD (24%). At increased potential difference of 60 volts, the onset time at cathode loop is seen to be longest (compared to lower potential) indicating waning of the impact of static potential in attracting ions/charged crystal cells. Similar phenomena could be observed at anode where the

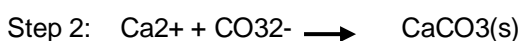
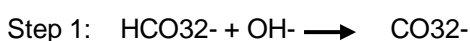
delaying effect is slightly less than the 40 volts experiment.

Impact of static potential on scale deposition time at higher temperature (90 oC) are presented in Table 2 and also graphically in Fig. 11 through Fig. 14. These results are in agreement with the known fact that CaCO₃ scaling is accelerated at increased temperature which is evident from the early onset of scale deposition in Set-B experiment compared to Set-A experiments. Scaling onset, both at cathode and anode loops are seen to be at or near 130 minute for the blank test conducted at 90 oC (Fig. 11). Compared to this, the scale deposition onset time is accelerated by 6% at cathode and decelerated by 38% at anode when 20 volts DC potential is applied (Table 2, Fig. 12). At increasing voltage (40 volts) the acceleration at cathode is not so significant (11% compared to the blank) however the deceleration at anode is more pronounced (54%). When the voltage was further increased to 60 volts, the impact on cathode is found to be less than 40 volts (8%) whereas further retardation is observed in anode loop (115% more than the blank test). It is also observable from this test data conducted at 90 oC that although there is irregularities in scaling onset at cathode, there is a linear relation with scale deposition delaying time and applied potential, which was not seen for low temperature experiments.

From the results of static and dynamic tests with experimental variables, it is clearly evident that the suspended CaCO₃ scale crystals are attracted towards the cathode, and repulsed at the anode resulting acceleration of scale deposition at the cathode tube and delaying of deposition inside the anode tube. Thus, it can be concluded that the suspended crystals or the crystals at their initial growth stage possess excess positive charge on the lattice surface, which is evidenced during ζ -potential measurements too.

IV. DISCUSSION

Numerous studies have been conducted on electro-migration and electro-deposition of CaCO₃ to derive the electrical properties of Calco-carbonate ions and the crystals in suspension. In case of electrodeposition, sufficient potential is applied on the electrode so that the dissolved molecular oxygen and water molecules are reduced at the cathode to produce hydroxyl ions (OH⁻) resulting in increased local pH upto 11 (Deslouis et al. 1997). This leads to the ion migration and precipitation of calcium carbonate on the electrode surface in the following two steps;



The kinetics of the above reaction is essentially driven by the current intensity and the convective diffusion rate of ions and molecular oxygen (Gabiellia et al. 1999).

Though in three of the 4 sets of dynamic flow results (cathode at 25 oC, anode at 25 oC and cathode at 90 oC) we did not find a clear pattern, but there are undeniable evidences that the scale deposition is accelerated in the cathode loop and retarded at the anode loop, essentially proving the movement of charged particles, either in ionic or in crystal form, though the electrical circuit is open and current flow was extremely low to be measured. Thus the mechanism responsible for the movement can be said to be of electro-phoresis, rather than electro-migration, as the electrodes are completely insulated from each other and the measured current flow was nearly negligible. Thus the observations in electrophoretic zeta potential measurement are of value to gain insight into the observed mechanism.

The structural defects of the crystal lattice due to random substitutions of one of the lattice ions by a foreign ion or random omissions, leaving an empty place in the crystal lattice could result in a residual electric charge. In addition to the defects, a crystal immersed in an electrolytic solution, may go through some ion exchanges with the solution it is immersed in. In aqueous solutions the charge associated on the surface are also attributed to hydrolysis or protonation, resulting in heterogeneities in the surface compared to the bulk crystal (Moulin and Roques, 2003). These associated electric charges generate a net surface force or electrostatic force. Though the absolute values of these forces are very small for matured crystals (compared to gravity), they can be of some significance when the surface area/volume ratio of the crystal is high, Which is the case when the crystals are at their nascent stage (very small and at suspension) This phenomenon, although is able to explain the movement of crystal cells towards a particular electrode, it alone cannot explain; (1) the preference of the moving charged particles towards cathode only and the repulsion felt at the anode. Excess charge on the crystal surface due to defect or ion exchange is not necessarily positive only. (2) It is difficult to explain the surface charge reversal observed during ζ -potential measurement using surface defect theory.

Simpson (1998), observed through FTIR & Raman spectra that the CaCO₃ scales deposited at low temperature (25 oC) on iron electrode is mostly "unstructured" CaCO₃ (similar to powdered CaCO₃) while at similar chemical environment the scale deposited at 90 oC are calcite in nature. In some cases proportion of calcite to veterite/aragonite increased with increasing temperature. Considering these results combined with the findings of Rodriguez-Blanco et al, (2012) and Bots et al, (2012), it would be reasonable to assume that calcite crystal formation occurs stepwise from amorphous (or unstructured) calcium carbonate, via the formation of vaterite which subsequently transforms themselves to calcite. At higher temperature this transformation process happens faster than at lower temperature, due to which only thermodynamically stable calcite crystals are observed in FTIR and Raman spectra for high

temperature measurements. From visual analysis of structure of the crystal cells, the Ca²⁺ density on the main basal planes (Figure 1, Table 1) and also the time dependent ζ -potential studies conducted in this work, it can be deduced that the unstable vaterite lattice possess a net positive charge. During the transformation to calcite they go through an ion transfer process and possess a net negative charge. By this time the crystals are large enough to overcome the weak electrostatic attraction-repulsion forces, gets into the influence of gravity and deposit on its flow path. The so called amorphous or unstructured materials formed at the very beginning, doesn't carry any net charge, possibility due the random orientation of the nascent crystal units in the agglomerates. In a nutshell, at the instant of mixing the two ion (Ca²⁺ and CO₃²⁻) the scale is in unstructured and charge neutral state, within few minutes they possess the vaterite structure with a net positive charge. At this stage they are relatively small and in suspension, thus able to migrate towards cathode and being repelled by the anode thus quickening the deposition process on the cathode tube wall, while delaying the deposition on the anode tube.

Relatively smooth pressure build up plots for higher temperature experiments and Shaw tooth type plots for the low temperature experiments also support this explanation. At low temperature, due to the delay of the transformation process from unstructured to vaterite to calcite, more unstructured material is depositing on the pipe wall rendering the deposits loosely bound. When sufficient pressure is developed they get expelled and the pressure fell. This resulted in Shaw tooth type pressure build up curve. Whereas at higher temperature, the crystals are quickly converted to regular shape calcite crystals rendering stronger bonding and low erosion, resulting in relatively smoother curves.

Comparing the difference of deposition time in cathode and anode with their respective blank experiments, it can be seen that retardation effect is more pronounced compared to acceleration effect. This can be explained from the fact that for accelerating the demotion kinetics, the charged particles has to travel towards the cathode surface overcoming the viscous drag force and the impact of gravity however small it may be. Whereas the retardation needs only to overcome the Van-der Walls attractive force.

From this study it can be inferred that even though it cannot be prevented completely, the deposition of CaCO₃ scale can be delayed significantly by applying static DC potential and converting the metal flow line into an anode. However, care has to be taken to counter the increased corrosion rate that may result due to conversion of metallic flow line into an anode.

V. CONCLUSIONS

Residual charge on the nascent CaCO₃ crystal nuclei and the impact of static electric potential on the deposition kinetics of the CaCO₃ scale is studied with

the help of static jar test, dynamic flow loop tests at variable temperatures and potential differences and also through electrophoretic ζ -potential studies.

It is seen that the deposition rate is accelerated at the cathode and retarded at the anode loop.

Retardation is more pronounced compared to acceleration and the impact of static potential is higher at higher temperature.

With the help of ζ -potential and flow study data it is concluded that the deposition at cathode is due to the initial unstable vaterite structure with a net positive charge.

It is also inferred that even though it cannot be prevented completely, the deposition of CaCO₃ scale can be delayed significantly by applying static DC potential and converting the metal flow line into an anode.

REFERENCES

- [1] V. Blanco-Gutierrez, A. Demourgues, V. Juberaab and M. Gaudon, "Eu(III)/Eu(II)- doped (Ca_{0.7}Sr_{0.3})CO₃ phosphors with vaterite/calcite/aragonite forms as shock/temperature detectors". *J. of Material Chem. C*. Vol. 2014(2), pp 9969-9977.
- [2] P. Bots, L.G. Benning, J.R. Blanco, T.R. Herrero and S. Shaw. "Mechanistic Insights into the Crystallization of Amorphous Calcium Carbonate (ACC)". *Crystal Growth & Design* Vol. 12(7), pp 3806–3814 (2012).
- [3] E Chibowski, L Hotysz and A Szczes, "Time dependent changes in ζ -potential of freshly precipitated CaCO₃". *Colloids and Surfaces A: Physicochem. Eng. Aspects*. Vol. 222 pp 41-54 (2003).
- [4] C. Deslouis, I. Frateur, G. Maurin and B. Tribollet (1997). "Interfacial pH measurement during the reduction of dissolved oxygen in a submerged impinging jet cell". *J. of Applied Electrochemistry* Vol. 27(4), pp 482-492.
- [5] G. Falini, S. Fermani, M. Gazzano and A. Ripamontia, "Polymorphism and architectural crystal assembly of CaCO₃ in biologically inspired polymeric matrices". *J. of Chem Soc., Dalton Trans.*, Vol. 2000, pp 3983-3987 (2000).
- [6] C. Gabriellia, G. Maurina, G. Poindessousa, R. Rosset "Nucleation and growth of CaCO₃ by an electrochemical scaling process". *J. of Crystal Growth*. Vol. 200(1–2), pp 236–250 (1999).
- [7] P. E. Hillner, A. J. Gratz, S. Manne and P. K. Hansma "Atomic-scale imaging of calcite growth and dissolution in real time". *Geology (Geological Society of America)* Vol. 20(4), pp 359-362 (1992).
- [8] P. Moulin, and H. Roques, " ζ -potential measurement of calcium carbonate". *J. of Colloid and Interface Science* Vol. 261, 115–126 (2003).

[9] L. Holysz, M. Chibowski, E. Chibowski, "Time-dependent changes of ζ -potential and other parameters of in situ CaCO_3 due to magnetic field treatment". *Colloids & Surfaces A: physicochemical and Engineering Aspects*. Vol. 208, pp 231–240 (2002).

[10] A. Pierre, J.M. Lamarche, R Mercier, "Calcium as potential determining ion in aqueous calcite suspensions". *J. of Dispersion Science and Technology*. Vol. 11(6), pp 611-635 (1990).

[11] J.D. Rodriguez-Blanco, S. Shawa and L.G. Benninga, "The kinetics and mechanisms of amorphous calcium carbonate (ACC) crystallization to calcite, via vaterite". *Nanoscale*. Vol. 3(1). pp 265–271 (2011).

[12] J.D. Rodriguez-Blanco, S. Shaw, P. Bots, T. Roncal-Herrero, L.G. Benning, "The role of pH and Mg on the stability and crystallization of amorphous calcium carbonate". *J. of Alloys and Compounds*. Vol. 536(1), pp 477–479 (2012).

[13] L.J. Simpson, "Electrochemically generated CaCO_3 deposits on iron studied with FTIR and Raman spectroscopy". *Electrochimica Acta*. Vol 43(16–17), pp 2543–2547 (1998).

Table 2. Summary of the experimental conditions and results of Dynamic Scale deposition studies

| PD (Volt) | <i>At cathode</i> | | <i>At anode</i> | |
|--------------------------|----------------------------|----------------------|----------------------------|-------------------|
| | <i>Scaling Onset (min)</i> | <i>% accelerated</i> | <i>Scaling Onset (Min)</i> | <i>% retarded</i> |
| Temperature 25 °C | | | | |
| 0 | 460 | - | 450 | - |
| 20 | 320 | 29 | 640 | 42 |
| 40 | 290 | 33 | 560 | 24 |
| 60 | 340 | 24 | 550 | 22 |
| Temperature 90 oC | | | | |
| 0 | 130 | - | 130 | - |
| 20 | 125 | 6 | 180 | 38 |
| 40 | 115 | 11 | 200 | 54 |
| 60 | 120 | 8 | 280 | 115 |

Table1. charge density of calcium ions (ions per nm^2) in different crystalline planes of calcium carbonate polymorphs

| | (001) Plane | (002) Plane | (100) Plane |
|------------------|--------------------|--------------------|--------------------|
| Calcite | 4.5 | 6.7 | - |
| Aragonite | 5.0 | - | - |
| Vaterite | 6.7 | - | 6.7 |

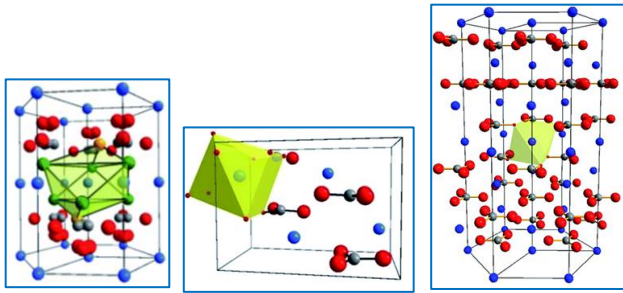


Fig. 1. Crystal lattice structure corresponding to (a) vaterite, (b) aragonite and (c) calcite allotropes. Blue sphere represent Ca^{2+} and red-grey unit represent CO_3^{2-} ions.

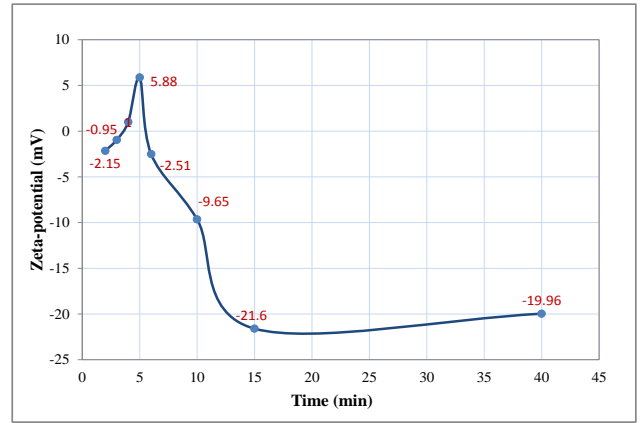


Fig. 5. Time dependent ζ -potential during the process of $CaCO_3$ crystal growth.

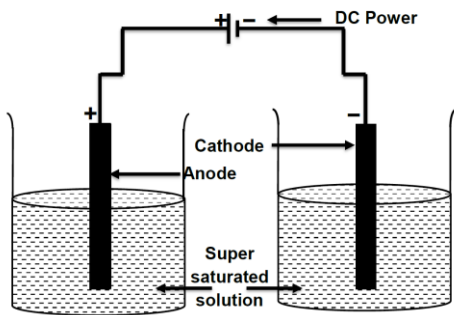


Fig. 2. Schematic of scale deposition experiments under static potential

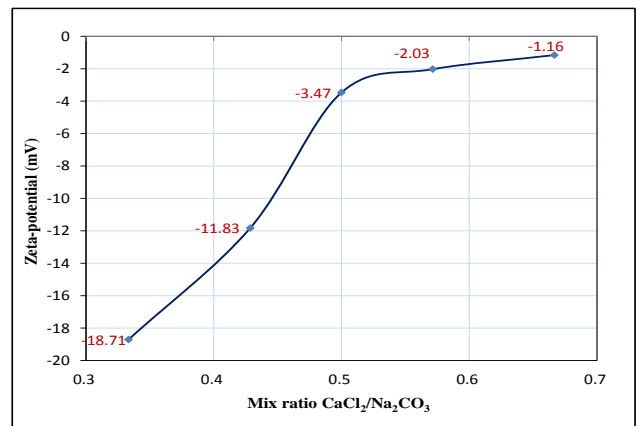


Fig. 6. ζ -potential of $CaCO_3$ crystal under various proportion of $CaCl_2$ and Na_2CO_3 .

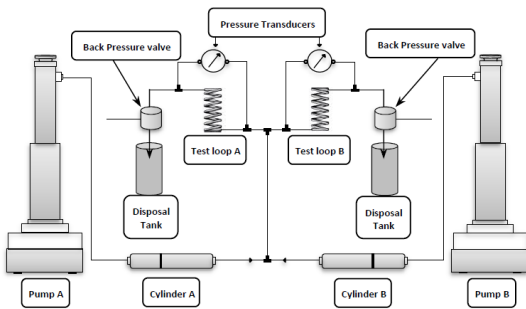


Fig. 3. Schematic of experimental setup for dynamic scale deposition study



Fig. 4. Photo image of the graphite electrodes (A) before and (B) after static scale deposition and confirmation test with HCl.

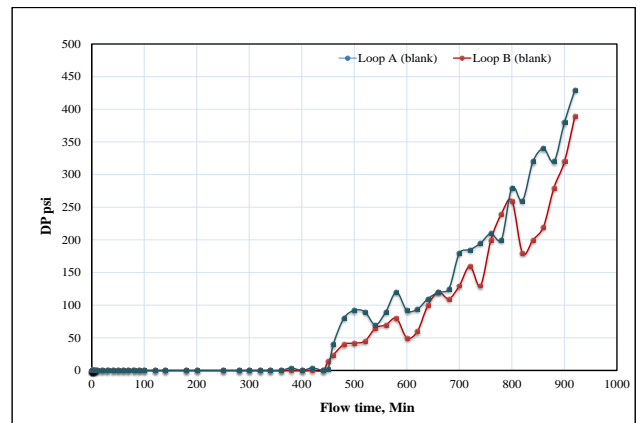


Fig. 7. Scale deposition behaviour at $25^\circ C$ – without static potential.

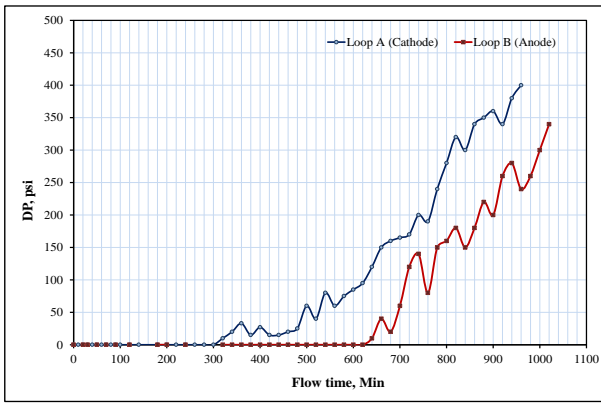


Fig. 8. Scale deposition behaviour at 25 °C under 20 volts potential difference.

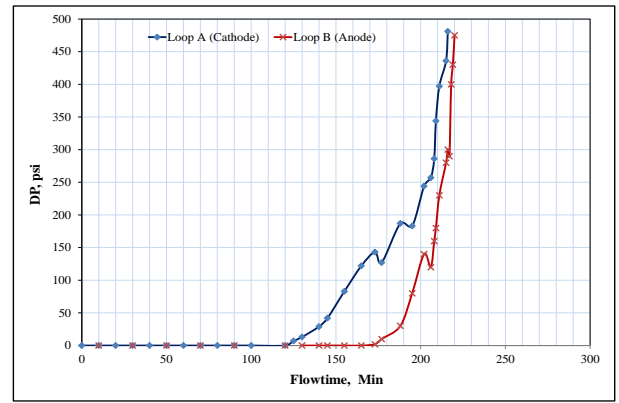


Fig. 12. Scale deposition behaviour at 90 °C under 20 volts potential difference.

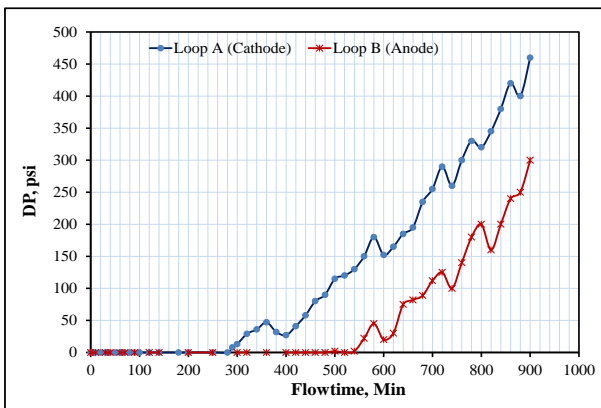


Fig. 9. Scale deposition behaviour at 25 °C under 40 volts potential difference.

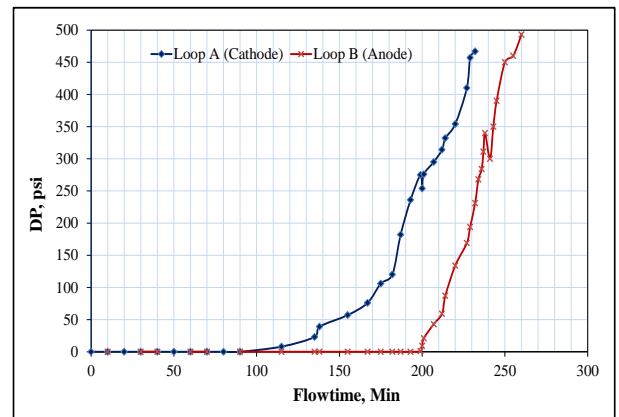


Fig. 13. Scale deposition behaviour at 90 °C under 40 volts potential difference.

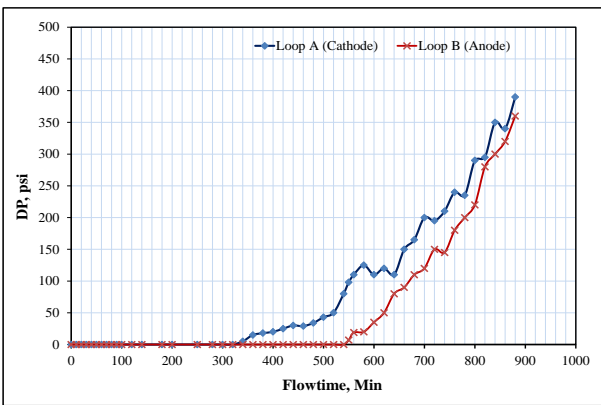


Fig. 10. Scale deposition behaviour at 25 °C under 60 volts potential difference.

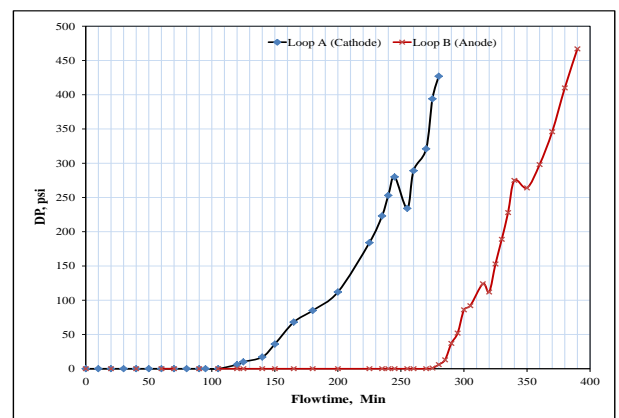


Fig. 14. Scale deposition behaviour at 90 °C under 60 volts potential difference.

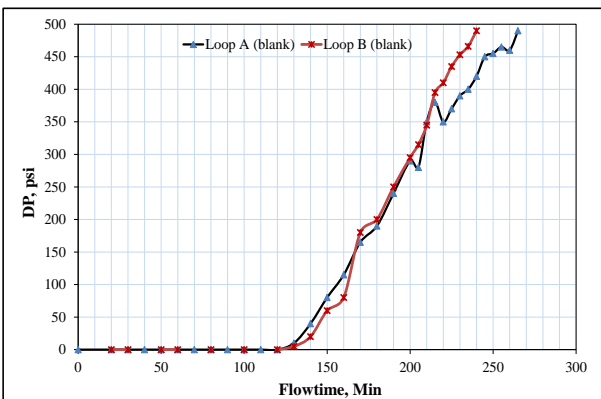


Fig. 11. Scale deposition behaviour at 90 °C (blank test)